



CHORUS

This is the accepted manuscript made available via CHORUS. The article has been published as:

Potential High-Performance Magnet: Fe- and Zr-Alloyed $\text{Ce}_{2}\text{Co}_{17}$

Tribhuwan Pandey and David S. Parker

Phys. Rev. Applied **13**, 034039 — Published 16 March 2020

DOI: [10.1103/PhysRevApplied.13.034039](https://doi.org/10.1103/PhysRevApplied.13.034039)

Potential high-performance magnet: Fe and Zr-alloyed $\text{Ce}_2\text{Co}_{17}$ *

Tribhuwan Pandey and David S. Parker

Material Science and Technology Division, Oak Ridge National Laboratory Oak Ridge 37831 TN USA

(Dated: February 12, 2020)

By performing comprehensive first principles calculations we study the hard magnetic properties of $\text{Ce}_2\text{Co}_{17}$ and $\text{Ce}_2\text{Fe}_{17}$ under Zr doping with varying Co concentration, given the substantial experimental success of Zr in improving magnetic anisotropy (MAE) in $\text{Ce}_2\text{Co}_{17}$ and $\text{Sm}_2\text{Co}_{17}$. We find that the magnetic properties of these alloys become comparable to state-of-the-art magnetic materials by doping with two elements Zr, and Fe, with potential energy products BH_{max} of 40 MG-Oe. The Zr substitution is particularly helpful for improving the MAE, leading to a magnetic hardness parameter $K_1/\mu_0 M_s^2$ significantly exceeding unity for a substantial range of Co concentration (between 60 and 100 percent of the $3d$ element concentration). The calculated MAE exhibits a strong dependence on Co concentration, indicative of a likely valence fluctuation with Co alloying, and shows a maximum value 7.78 MJ/m^3 for 60 % Co doping. Thus upon experimental verification these alloys may become competitors to the better known permanent magnet materials $\text{Nd}_2\text{Fe}_{14}\text{B}$ and SmCo_5 .

I. INTRODUCTION

Strong permanent magnets are indispensable for industrialized society, finding myriad applications in sectors ranging from the automotive (for both electrified and petroleum-fueled vehicles) to power generation (such as wind turbine generators) to computer hard disk drives to electric motors. The search for new and improved strong permanent magnets is therefore a substantial topic of worldwide research today, with numerous national and international efforts worldwide. Reducing the rare earth content in the state-of-the-art permanent magnets (such as $\text{Nd}_2\text{Fe}_{14}\text{B}$) is of particular interest and is a commonly used strategy. The most notable examples are reducing Neodymium content in $\text{Nd}_2\text{Fe}_{14}\text{B}$ by doping with La or Ce at Neodymium site¹⁻⁴. Another possible design scenario is *rehabilitation* of seemingly unpromising materials into high performance magnets by elemental substitution, the tuning of composition, interstitial modifications or other means. For example recent experimental and theoretical studies^{5,6} show that paramagnetic CeCo_3 can be transformed into a potential permanent magnet by Mg alloying. Ce is a rather abundant and therefore relatively inexpensive rare earth, so that Ce based magnetic compounds are attractive for permanent magnet application if sufficient magnetic anisotropy can be attained.

Ce forms many interesting magnetic compounds with the transition metals Fe, and Co such as CeCo_5 , $\text{Ce}_2\text{Fe}_{17}$, and $\text{Ce}_2\text{Co}_{17}$. Among these CeCo_5 has shown potential for possible applications due to its relatively high Curie point (653 K) and large uniaxial magnetic anisotropy (9.5 MJ/m^3)^{7,8}. $\text{Ce}_2\text{Co}_{17}$ on the other hand, despite its very high Curie point (1023 K) and large saturation moment (1.1 T), remains a rather inferior magnet due to its rather small uniaxial magnetic anisotropy energy (MAE). It was previously shown that, the poor MAE of R_2Co_{17} compounds stems from the negative contribution of the Co atoms occupying the “dumbbell” site in the rhombohedral structure⁹. After that many experimental studies have explored the possibility of improving the MAE of this material by substitutions at this dumbbell site by using Fe¹⁰, Mn^{10,11}, Zr^{10,12}, Si¹³, and Al^{14,15}. Among these the maximum MAE was observed for Zr doped $\text{Ce}_2\text{Co}_{17}$. By studying $\text{Sm}_2\text{Co}_{17}$ Larson *et.al*¹⁶ showed that the MAE of 2-17 magnetic compounds can be significantly improved by Zr substitu-

tion for dumbbell site Co atoms (1 Zr \rightarrow 2 Co). This huge increase in MAE originates from a substantial lattice relaxation upon Zr alloying, which makes the Sm-Co distances comparable to the corresponding values in the very high MAE material ($K_1 = 17.2 \text{ MJ/m}^3$) SmCo_5 . This concept was recently extended to $\text{Ce}_2\text{Co}_{17}$ by Ke *et.al*¹⁷, where they reported 10 times enhancement in MAE by Zr substitution.

There is however a substantial downside of this substitution at the dumbbell site — a penalty to the magnetization. The highest magnetic moment for Co atoms in the $\text{Ce}_2\text{Co}_{17}$ rhombohedral structure is observed at the dumbbell site, and substitution of non magnetic Zr reduces the already relatively poor magnetic moment drastically. Therefore for possible permanent magnet applications the magnetic moment of $\text{Ce}_2\text{Co}_{15}\text{Zr}$ needs to be improved. Here, by performing state-of-the-art first principles density functional theory calculations we propose a possible solution of this problem in the $\text{Ce}_2\text{ZrFe}_{15-x}\text{Co}_x$ alloy. We begin with $\text{Ce}_2\text{Fe}_{17}$, a compound with a $\sim 50\%$ larger total magnetization than $\text{Ce}_2\text{Co}_{17}$, though it suffers from planar MAE (and is in fact a helimagnet rather than a ferromagnet) which does not change its sign even after Zr substitution at dumbbell site. By substituting Co for Fe, we report that MAE can be tuned to a very large uniaxial value of 7.78 MJ/m^3 at 60%, Co alloying with relatively little sacrifice in magnetic moment. We assess that this enhancement in MAE is related to Ce valence fluctuations in these compounds. From our electronic structure analysis, we conclude that for Co concentration equal to or higher than 40%, Ce changes its valency from tetravalent to trivalent leading to a transition from planar to uniaxial behavior and thereby a strong enhancement in the MAE.

II. METHODOLOGY

All first principles calculations were performed within density functional theory (DFT) using the general potential linearized augmented plane-wave (LAPW) method + local orbitals^{18,19} as implemented in the WIEN2K code²⁰. The LAPW sphere radii were set to 2.30 Bohr for Ce and 1.83 Bohr for Fe, Co and Zr. In addition, RK_{max} (the product of the smallest LAPW sphere radius (R) and the interstitial plane-wave cut-

off, K_{max}) of 9.0 is used to ensure a well-converged basis set. The calculations for $\text{Ce}_2\text{Fe}_{17}$, and $\text{Ce}_2\text{Co}_{17}$ were performed using the experimental lattice parameters with internal coordinates relaxed. It was shown that upon Zr substitution at the dumbbell site (1 Zr \rightarrow Co₂ or Fe₂) the volume of the unit changes by less than 2%. The calculations for $\text{Ce}_2\text{Fe}_{15}\text{Zr}$ and $\text{Ce}_2\text{Co}_{15}\text{Zr}$ were also performed at the experimental lattice parameters of the corresponding base compounds. The Co alloying at selected concentrations between $\text{Ce}_2\text{Fe}_{15}\text{Zr}$ and $\text{Ce}_2\text{Co}_{15}\text{Zr}$ was modeled within virtual crystal approximation (VCA). For the alloyed system $\text{Ce}_2\text{Fe}_{15-x}\text{Co}_x\text{Zr}$ the lattice parameters were modified according to Vegard's law^{21,22}. For all the systems internal atomic coordinates were determined by minimizing the total energy using the generalized gradient approximation (GGA) of Perdew and co-workers²³ until forces on all the atoms were less than 1 mRy/Bohr. For this purpose 1000 reducible \mathbf{k} -points were used in the full Brillouin zone. Although VCA correctly predicts the magnetic moments it can overestimate the MAE. To address this issue the Co doping in $\text{Ce}_2\text{Fe}_{15}\text{Zr}$ was also studied using the supercell method.

For the calculation of magnetic crystalline anisotropy (MAE), spin-orbit coupling was included within the standard second variational approach²⁴. MAE calculations were performed by using 5000 \mathbf{k} -points. To check the convergence of MAE with respect to the number of \mathbf{k} -points additional calculations were performed with 4000 \mathbf{k} -points. Upon this change, the MAE varies only by approximately 3%, demonstrating the excellent convergence of these calculations. All the calculations presented here correspond to 5000 \mathbf{k} -points in the entire Brillouin zone. As is well known, the magnetic character of Ce (localized vs itinerant) in particular for Ce and transition metal compounds is debatable. Often pressure, chemical substitution can induce itinerant to localized crossover^{25,26}. The widely used extension of DFT which can effectively describe electron localization are the self-interaction corrected-local spin density approximations (SIC-LSD)²⁷ and DFT+U methods²⁸. In the SIC-LSD method^{27,29,30} the total energy is corrected for spurious self-interaction of each localised state, and this corrections vanishes for an itinerant state. In the DFT+U method a quadratic correction energy (which includes the Hubbard repulsion and double counting term) is added to the Hamiltonian for better description of the correlated f electrons. For the localized case, in our calculations the rare earth f orbitals are described within the DFT+U formalism which adds a Hubbard U parameter and the Hund's coupling parameter J to split the localized f orbitals above and below the Fermi level. The Coulomb correlations within the Ce-4 f localized orbitals were described using the the self-interaction correction scheme³¹⁻³³, which only depends on $U_{\text{eff}} = U - J$. Here as in our previous work⁴ a value of $U - J = 3$ eV for Ce was used. The density of states and magnetic properties from both GGA+SOC, and GGA+SOC+U calculations are compared.

III. RESULTS AND DISCUSSION

A. Effect of Zr substitution on magnetic properties of $\text{Ce}_2\text{Fe}_{17}$ and $\text{Ce}_2\text{Co}_{17}$

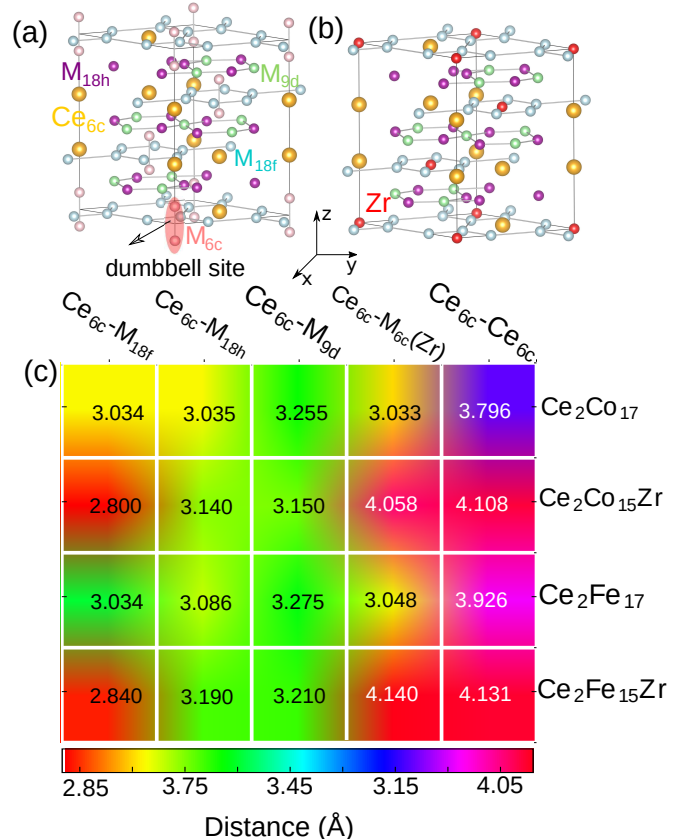


FIG. 1. (a) Rhombohedral crystal structure of Ce_2M_{17} ($M = \text{Co}$ or Fe) unitcell, with all the crystallographic Wyckoff sites denoted by corresponding atomic site colors. (b) Crystal structure of $\text{Ce}_2\text{M}_{15}\text{Zr}$ after substituting one Zr atom (shown in red color) for two dumbbell site M atom (Fe(Co)-6c site shown by shaded area in (a)). (c) The nearest neighbor (NN) Ce-M, and Ce-Zr distances in Ce_2M_{17} , and $\text{Ce}_2\text{M}_{15}\text{Zr}$. Here M refers to either Fe or Co. For comparison first two Ce nearest neighbor distances in CeFe_5 and CeCo_5 are 2.806Å; 3.147Å, and 2.845Å; 3.179Å, respectively.

We begin by calculating the magnetic properties of the base compounds $\text{Ce}_2\text{Fe}_{17}$, and $\text{Ce}_2\text{Co}_{17}$. Note that for the purposes of this work we model $\text{Ce}_2\text{Fe}_{17}$ as a ferromagnet, despite the experimental presence³⁴⁻³⁸ of helimagnetism; as we find the region of interest for permanent magnets to be generally on the Co-rich side of these compositions (where ferromagnetic behavior indeed prevails), this does not introduce appreciable error. To estimate the magnetic ground state for $\text{Ce}_2\text{Fe}_{15-x}\text{Co}_x\text{Zr}$ alloys at various Co concentrations we did calculations of several collinear spin configurations as discussed in the Supplemental Material³⁹. Energetic of these configurations are given in Table S1, which illustrates that the ferromagnetic configuration where all Fe/Co atoms are

TABLE I. The calculated spin magnetic moments at various atomic sites, total (spin + orbital) magnetic moment and magnetic anisotropy calculated within the GGA by including spin orbit coupling with a Hubbard U parameter of 3 eV at Ce site. Calculation for $\text{Ce}_2\text{Fe}_{17}$ and $\text{Ce}_2\text{Co}_{17}$, (and corresponding Zr doped compounds) were performed at the experimental lattice parameters adopted from references³⁷, and ¹⁰, respectively. The calculated formation energies (E^{for}) with respect to elemental decomposition are also shown. The E^{for} is calculated without spin orbital coupling and without U. For the alloyed systems lattice parameters were scaled according to Vegard's law. All the lattice parameters employed in our work are listed below. Here Cobalt doping was performed within virtual crystal approximation.

Parameter	Compounds							
	$\text{Ce}_2\text{Fe}_{17}$	$\text{Ce}_2\text{Fe}_{15}\text{Zr}$	$\text{Ce}_2\text{Fe}_{12}\text{Co}_3\text{Zr}$	$\text{Ce}_2\text{Fe}_9\text{Co}_6\text{Zr}$	$\text{Ce}_2\text{Fe}_6\text{Co}_9\text{Zr}$	$\text{Ce}_2\text{Fe}_3\text{Co}_{15}\text{Zr}$	$\text{Ce}_2\text{Co}_{15}\text{Zr}$	$\text{Ce}_2\text{Co}_{17}$
a (Å)	8.489	8.489	8.468	8.447	8.425	8.404	8.383	8.383
c (Å)	12.408	12.408	12.371	12.334	12.297	12.260	12.223	12.223
$\mu_{\text{Ce-(6c)}} (\mu_B)$	-0.66	-0.48	-0.52	-0.92	-0.90	-0.85	-0.80	-0.96
$\mu_{\text{Zr}} (\mu_B)$	-0.27	-0.28	-0.28	-0.28	-0.27	-0.24		
$\mu_{\text{Fe/Co-(6c)}} (\mu_B)$	2.56							1.70
$\mu_{\text{Fe/Co-(9d)}} (\mu_B)$	2.05	2.04	2.17	2.05	1.91	1.73	1.54	1.08
$\mu_{\text{Fe/Co-(18f)}} (\mu_B)$	2.36	2.20	2.14	2.02	1.85	1.64	1.41	1.60
$\mu_{\text{Fe/Co-(18h)}} (\mu_B)$	2.22	2.13	2.20	2.10	1.94	1.75	1.54	1.56
$M_{\text{TOT}} (\mu_B/\text{per u.c.})$	38.04	30.26	30.77	28.92	27.15	24.12	21.14	25.88
K_1 (MJ/m ³)	-1.97	-5.54	-5.36	2.23	7.78	5.17	4.67	0.40
E^{for} (meV/atom)		-44.0	-80.0	-88.0	-110.0	-114.0	-112.0	

aligned in the same directions is energetically most favorable. This ferromagnetic behaviour of $\text{Ce}_2\text{Fe}_{15-x}\text{Co}_x\text{Zr}$ alloys is supported by the previous experimental study of Shaheen *et. al.*⁴⁰ which finds that $\sim 10\%$ Co alloying in $\text{Ce}_2\text{Fe}_{17}$ yields a substantial room-temperature magnetization, or in other words a ferromagnet, as we have assumed. Additionally, the previous studies^{10,12} on ferromagnetic $\text{Ce}_2\text{Co}_{17}$ finds that under Zr alloying this material remains ferromagnetic. These facts together strongly suggest that the ground state of our Fe and Zr-alloyed $\text{Ce}_2\text{Co}_{17}$ material is in fact a ferromagnetic one.

The calculated magnetic moments and MAE values for $\text{Ce}_2\text{Fe}_{17}$ and $\text{Ce}_2\text{Co}_{17}$ are listed in Table I. For $\text{Ce}_2\text{Co}_{17}$ the calculated total (spin + orbital) magnetization of 25.88 μ_B per formula unit is in very good agreement with the measured value of 26.6 μ_B ^{10,12}. Similar to numerous other rare earth magnets^{4,6,41} the Ce spin magnetic moment prefers to be anti-aligned with respect to Co with an average spin moment of $-0.66\mu_B$, and $-0.96\mu_B$ for the Fe and Co end-members, respectively. In accordance with Hund's third rule, the Ce orbital moment is anti-parallel with spin moment. For $\text{Ce}_2\text{Co}_{17}$ our calculations find a small uniaxial magnetic anisotropy of ~ 0.4 MJ/m³ from DFT+U calculations, which is in excellent agreement with the 5K measured experimental value of 0.55 MJ/m³^{10,12}. By omitting Hubbard U from our calculations, a MAE value of 0.44 MJ/m³ was obtained, which is comparable with the MAE obtained from DFT+U calculations with $U_{\text{Ce}} = 3\text{eV}$.

This MAE value is substantially lower than the ~ 4.5 MJ/m³ MAE for the state of the art permanent magnet $\text{Nd}_2\text{Fe}_{14}\text{B}$ and renders this material unsuitable as a hard permanent magnet. The most promising way for enhancing the MAE of 2-17 magnets was proposed by Larson *et. al.*¹⁶ in $\text{Sm}_2\text{Co}_{17}$. They suggested that the MAE of $\text{Sm}_2\text{Co}_{17}$ may become comparable to SmCo_5 by a single Zr substitution for two Co "dumbbell" site atoms. Such a substitution is sensible

considering the more than twice larger atomic volume of Zr relative to Co. This was later confirmed in $\text{Ce}_2\text{Co}_{17}$, by Ke *et. al.*¹⁷ where by Zr doping at the dumbbell site they reported a significant enhancement in MAE. Here for completeness we recalculate the magnetic properties of $\text{Ce}_2\text{Fe}_{17}$ and $\text{Ce}_2\text{Co}_{17}$ under Zr substitution, which are described in Table I.

First we discuss effect of Zr substitution on the structural and magnetic properties of $\text{Ce}_2\text{Fe}_{17}$ and $\text{Ce}_2\text{Co}_{17}$. The nearest neighbor (NN) distances between Ce and various M (Co/Fe) Wyckoff sites with and without Zr substitution are shown via a heat-map in Figure 1(c). In the base structure Ce_2M_{17} ($\text{Ce}_2\text{Fe}_{17}$ or $\text{Ce}_2\text{Co}_{17}$) the NN distances between Ce_{6c} and M_{18f} , M_{18h} , M_{6c} sites are comparable, followed by the Ce_{6c} - M_{9d} distance. Upon Zr substitution at the Ce_2M_{17} (M = Fe, Co) dumbbell site shown by the red shaded ellipse in Figure 1 (a), the distance between Ce_{6c} and M_{18f} site is significantly decreased. A reduction can also be seen in the distances between the Ce_{6c} and M_{9d} -sites. Whereas the distances between Ce_{6c} - M_{18h} and Ce_{6c} - Ce_{6c} sites increase. In particular these Ce-NN distances are comparable to those in CeFe_5 ($1^{st}_{NN} : 2.806\text{\AA}$; $2^{nd}_{NN} : 3.147\text{\AA}$) and CeCo_5 ($1^{st}_{NN} : 2.845\text{\AA}$, $2^{nd}_{NN} : 3.179\text{\AA}$). This is consistent with the structure relaxation effects reported in $\text{Sm}_2\text{Co}_{17}$ under Zr doping¹⁶. We observed that on $\text{Co}_2 \rightarrow \text{Zr}$ substitution the spin magnetic moment of the Co_{9d} site increases by 0.46 μ_B to 1.54 μ_B , and the moment on the Co_{18f} site decreases by 0.19 μ_B . As expected, due to substitution of a non-magnetic element the total magnetic moment for $\text{Ce}_2\text{Co}_{15}\text{Zr}$ reduces to 21.14 μ_B per formula unit.

In agreement with previous studies, our results find that for $\text{Ce}_2\text{Co}_{15}\text{Zr}$ the MAE increases to 4.67 MJ/m³, which is ten times higher than the corresponding value for $\text{Ce}_2\text{Co}_{17}$. By analyzing the contribution from crystallographic sites Ke *et. al.*¹⁷ proposed that Zr substitution at the dumbbell site eliminates the negative contribution from the Co dumbbell

sites, which results in huge MAE. Previously many experimental studies have investigated the effect of various transition metal atom doping such as Zr, Hf, Ti, V, Cr, Mn, Fe, and Cu on the Co site¹⁰⁻¹⁵. Among these the highest enhancement in anisotropy field was found for Zr doping at Co site^{10,12}. By performing structural analysis Wallace and co-workers^{10,12} showed that upon Zr substitution the volume (per formula unit) of $\text{Ce}_2\text{Co}_{17}$ increases slightly from 247.5 \AA^3 to 249.4 \AA^3 . Since the atomic radius of Zr is larger than Co and smaller than Ce, this volume enhancement suggests that Zr prefers to substitute for Co atoms. Note that this volume increase is driven by the increase in in-plane lattice parameter a and a small decrease in out of plane lattice parameter c , implies that Zr substitution at dumbbell site is preferred. This claim can be further validated by comparing the measured and calculated magnetic properties. The experimental measurements^{10,12} for a sample of stated composition $\text{Ce}_2\text{Co}_{16}\text{Zr}$ show a MAE of 3.13 MJ/m^3 and saturation magnetization of $20 \mu_B$ per formula unit at 77 K. These values are captured in our calculations ($M_s = 21.72 \mu_B$ per formula unit, and MAE = 4.67 MJ/m^3) where one Zr atom replaces Co_2 dumbbell ($\text{Zr} \rightarrow \text{Co}_2$). Note that the calculated¹⁷ magnetic properties by replacing both Co_2 dumbbell atoms by Zr atoms is only 0.95 MJ/m^3 . This is much smaller than the measured experimental value and strongly suggests that Zr most likely substitutes for 2 Co at the dumbbell site, as we and previous authors assume.

B. Magnetic properties of $\text{Ce}_2\text{ZrFe}_{15-x}\text{Co}_x$ alloys

As described above although the MAE of $\text{Ce}_2\text{Co}_{17}$ can be improved by Zr substitution, it significantly reduces the magnetization. Next, we investigate the possibility of improving the magnetic properties of $\text{Ce}_2\text{Fe}_{15}\text{Zr}/\text{Ce}_2\text{Co}_{15}\text{Zr}$ by Co/Fe alloying. Magnetic properties as a function of various composition ranges between $\text{Ce}_2\text{Fe}_{15}\text{Zr}$ and $\text{Ce}_2\text{Co}_{15}\text{Zr}$ were studied within the virtual crystal approximation (VCA). Within VCA the random atom occupation between two types of atoms is treated by using an averaged charge virtual atom. In order to model the alloyed compound the lattice parameters within the composition range were scaled according to Vegard's law²², which are listed in Table I. Using these lattice parameters at each alloy composition the atomic positions were optimized until forces were less than 1 mRy/Bohr . The computed magnetic properties at various Co concentrations are listed in Table I. The total magnetization and MAE as a function of Co doping (x) is plotted in Figure 2(a) and Figure 2(b), respectively. Here results of both without U and with $U_{\text{Ce}} = 3 \text{ eV}$ calculations are shown. As shown in Figure 2(a), while with Co doping the total magnetic moment of system in general decreases, it still maintains a significant value of $27.15 \mu_B$ per formula unit for $\text{Ce}_2\text{Fe}_6\text{Co}_9\text{Zr}$ alloy. This value of total magnetic moment is only 1.1 times smaller than that of the end member compound $\text{Ce}_2\text{Fe}_{15}\text{Zr}$, and 1.3 times higher than the magnetic moment of $\text{Ce}_2\text{Co}_{15}\text{Zr}$. We find that for $\text{Ce}_2\text{ZrFe}_{15-x}\text{Co}_x$, when Co doping is less than 40% ($x < 6$) the MAE remains planar, and as the Co substitution exceeds 40% ($x > 6$) the MAE switches to uniaxial. The highest uni-

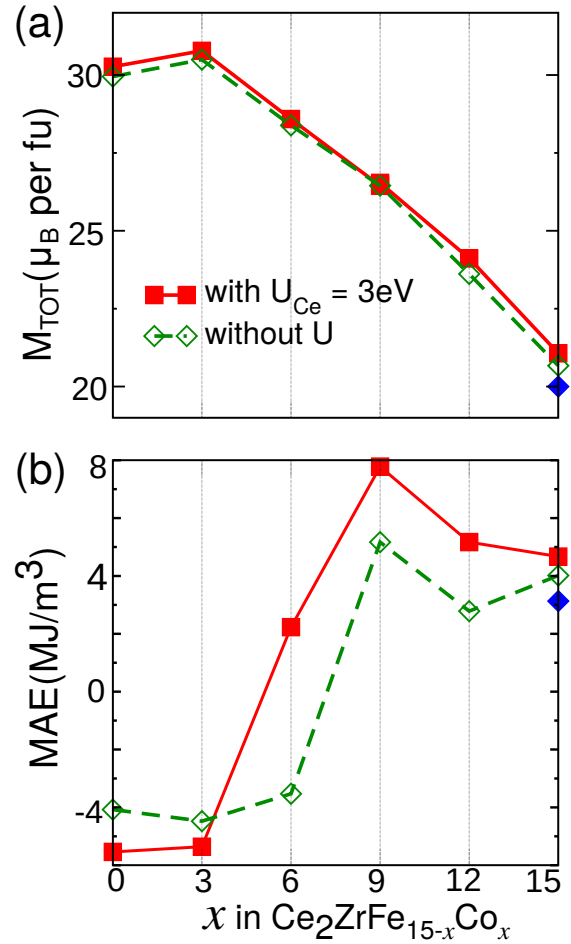


FIG. 2. (a) Total magnetic (spin + orbital) moment and (b) magnetic anisotropy energy in $\text{Ce}_2\text{ZrFe}_{15-x}\text{Co}_x$ as function of x . Here the Co doping is performed under virtual crystal approximation (VCA). Symbols correspond to the calculated compositions, and the line is a guide to eye. The blue diamonds represent experimental data from Refs.^{10,12}. Results from both without Hubbard U (open green diamonds) and with Hubbard $U_{\text{Ce}} = 3 \text{ eV}$ (red filled squares) calculations are compared here.

axial anisotropy, with MAE = 7.78 MJ/m^3 occurs for 60% Co doping in $\text{Ce}_2\text{Fe}_6\text{Co}_9\text{Zr}$ alloy. This MAE is 1.6 times larger than the MAE of $\text{Ce}_2\text{Co}_{15}\text{Zr}$. These calculated properties show that $\text{Ce}_2\text{ZrFe}_{15-x}\text{Co}_x$ alloys may exhibit performance comparable to the state of art permanent magnets. As shown in Figure 2(b) the enhancement of MAE was also observed in the calculations without Hubbard U parameter. Although the MAE is relatively smaller compared to Hubbard U_{Ce} calculation, it is still sufficiently large (at 5.16 MJ/m^3 for the 60 percent Cobalt case) for a strong permanent magnet, given the magnetic hardness parameter $\kappa = K_1/\mu_0 M_s^2$ of 4.05 even at this lesser MAE value. Additionally, along with Ce f -electrons we also explore the effect of localization on Co d -electrons. For this GGA+ U calculations were performed for the Co end member ($\text{Ce}_2\text{ZrCo}_{15}$) and 60% Co doped case ($\text{Ce}_2\text{ZrFe}_6\text{Co}_9$), using a U of 3 eV on Co as well

as on Ce, in addition on Co alone. However, as described in Table S2 of the Supplemental Information³⁹, this yields unphysically large MAE values exceeding 30 MJ/m³ for the experimentally known end-member case (experimental measurements^{10,12} for Ce₂Co₁₆Zr show a MAE of 3.13 MJ/m³ at 77 K). Therefore, we consider that any effects of Co localization are not sufficient to warrant applying the GGA+U approach to the Co atom itself. It is noteworthy that while the MAE values calculated with and without Hubbard U are a bit different (particularly at 60 % Co doping), they follow the same qualitative trend. Besides, our previous studies on Ce-Co compounds — Ce₂Co₉Mg^{5,6}, and CeCo₅⁸ show that localized treatment of Ce-*f* electrons is important in order to obtain correct MAE. For example, the MAE for Ce₂Co₉Mg calculated without Hubbard U is only 0.46 MJ/m³ much smaller than the experimental MAE value of 2.2 MJ/m³. By including U_{Ce} = 1.5 eV, MAE of 2.10 MJ/m³ was obtained which is in excellent agreement with the experimental data. Similarly, for CeCo₅ the MAE calculated without Hubbard U is 3.17 MJ/m³; smaller than experimental value of 10.5 MJ/m³. However a DFT + U calculations with U_{Ce} = 3.0 eV gives a MAE of approximately 9.0 MJ/m³, which is in good agreement with the experimental value. These results suggest the likelihood of substantial localization of Ce *f* electrons in Ce-Co compounds.

Next in order to understand this enhancement in MAE we analyze the density of states (DOS) at various Co concentrations in Ce₂ZrFe_{15-x}Co_x which are shown in Figure 3(a)-(e). The DOS near the Fermi level predominantly originates from Ce *f*- and Fe/Co *d*-states. As shown in Figure 3, the Ce-*f* states are (black orange filled lines) partially occupied in the spin-down channel, and empty in the spin-up channel, confirming that the Ce spin moment anti-aligns with Fe/Co spin moments. The enhanced ($\times 15$) Zr DOS (red dashed line) is also shown for comparison. Although the Zr DOS at Fermi level is relatively small, there is some hybridization present with the neighboring Ce and Co atoms. The magnetic properties of Ce-transition metal compounds are shown to be sensitive to the valence of Ce^{11,42-45}. Though, the accurate Ce-*f* valence in Ce-transition metal is still debatable, previous studies report the occurrence of mixed Ce valency⁴⁴⁻⁴⁸. In particular for Ce₂Fe₁₇, and Ce₂Co₁₇, the X-ray absorption spectroscopy analysis suggests a Ce valence between 3.0 to 3.3^{44,45}.

Perhaps the most intriguing feature of the DOS is the modification of the Ce valence by varying Co concentration which is clearly demonstrated in Figure 4(a). The DOS for three representative cases (Ce₂Co₁₅Zr, Ce₂ZrFe₆Co₁₅, and Ce₂Co₁₅Zr) with U_{Ce} = 3eV, and without U is compared in Figure S2 of Supplemental Material³⁹. For Ce₂ZrFe_{15-x}Co_x, when the Co doping is less than 40 % ($x < 6$) the main localized Ce-*f* states are situated above the Fermi level with the band tail extending below Fermi level. This indicates tetravalency of Ce in these particular alloys. As the Co doping exceeds 40% ($x > 6$), some of these localized Ce-*f* states shift below the Fermi level, which should correspond to trivalent Ce. While the occupied 4*f* peak appearing for 40% and greater Cobalt concentration is relatively small, its presence

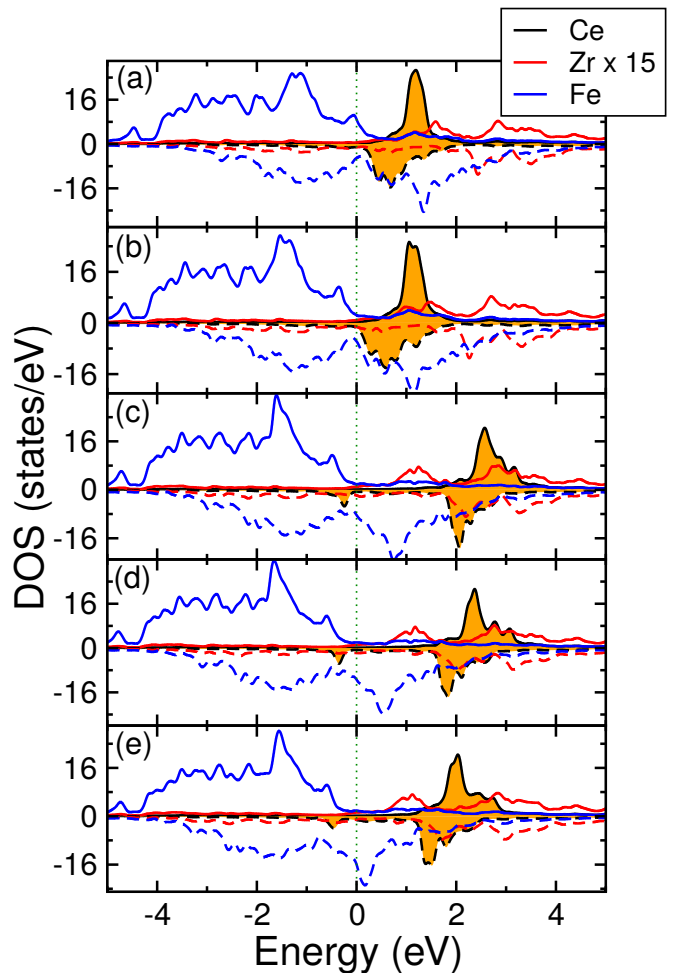


FIG. 3. The Ce *f* (black and orange filled lines), and Co+Fe *d*, DOS (blue lines), Zr DOS (red lines) in (a) Ce₂Fe₁₅Zr, (b) Ce₂Fe₁₂Co₃Zr, (c) Ce₂Fe₉Co₆Zr, (d) Ce₂Fe₆Co₉Zr, and (e) Ce₂Co₁₅Zr calculated within GGA+SOC+U. The Zr DOS is enlarged by 15 times for clarity. The Co/Fe DOS is averaged over all Co and Fe atoms. The spin-up and spin-down states are shown by positive and negative, respectively.

is sufficient to yield large increases in the magnitudes of both the Cerium spin and orbital moments (see Figure 4(b)), which ultimately yield the large MAE. This switching of Ce valency on Co concentration can be correlated with calculated Ce spin (M_{SPIN}) and orbital magnetic moments (M_{ORB}), which are shown on the left and right y-axis in Figure 4(b). As the Ce-valency switches from tetravalent (Ce⁴⁺) to trivalent (Ce³⁺) both spin and orbital magnetic moment exhibit significant increases. For example in Ce₂ZrFe₁₅ (where Ce is in tetravalent state) the spin and orbital moments are $-0.48\mu_B$ and $0.18\mu_B$, respectively. For 40% Co doping the Ce spin and orbital moments increase (in magnitude) to $-0.92\mu_B$ and $0.57\mu_B$. This behavior is consistent with the fact that the Ce³⁺ is more magnetic than Ce⁴⁺. Though the reason for the appearance of this 4*f* peak remains unclear, previous reports^{25,26} has shown that the itinerant or localized nature of Ce, can be sensitive to the

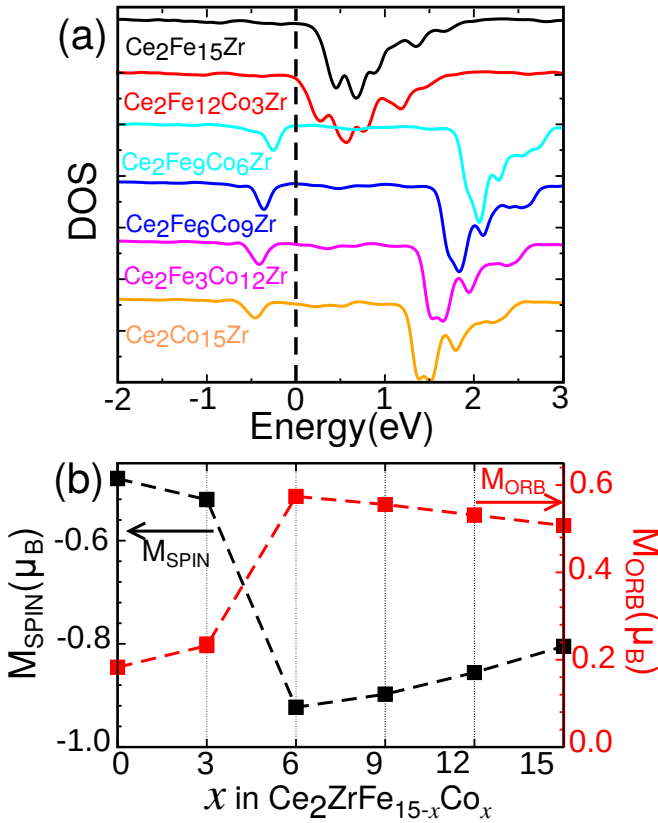


FIG. 4. (a) The modification in Ce spin-down f DOS on going from $\text{Ce}_2\text{Fe}_{15}\text{Zr}$ to $\text{Ce}_2\text{Co}_{15}\text{Zr}$ at various Co concentrations calculated under GGA+SOC+U. For 40% Co concentration ($\text{Ce}_2\text{Fe}_9\text{Co}_6\text{Zr}$) and on-wards the valency of Ce switches from tetravalent to trivalent. For clarity, the DOS plots have been shifted with respect to one another. The Ce valency transition is also reflected in the Ce spin (M_{SPIN} ; marked on left y-axis) and orbital (M_{ORB} ; marked on right y-axis) moments shown in (b), where a abrupt increase is observed for 40% Co concentration.

volume, surrounding local environment, and chemical substitution. This suggests that the $4f$ peak for $\text{Ce}_2\text{ZrFe}_{17-x}\text{Co}_x$ alloys can be attributed to volumetric, or chemical pressure effect associated with the 4% smaller volume of the end-member Co compound, relative to the Fe end member as shown in Table I. Though we do not confirm the possibility of valence fluctuation, the sharp increase in magnetic anisotropy energy along with magnetic moments supports our hypothesis of Ce-valence fluctuation as a function of Co concentration in these alloys.

To explain the calculated enhancement of magnetic properties next we analyze the anisotropy of the orbital magnetic moment. The Ce and Fe/Co orbital magnetic moments along the in-plane (a -axis), and out-of-plane (c -axis) directions are plotted in Figure 5(a), and (b), respectively. The Co/Fe orbital magnetic moments are averaged over all the sites. The anisotropy of orbital moments (ΔM_{ORB}) is computed by taking the difference between orbital magnetic moment along c , and a direction. Both Ce and Fe/Co site exhibit substantial orbital magnetic anisotropy, which increases with Co concen-

tration. With increasing Co doping the relatively small value of $M_{\text{ORB}}^{\text{Ce}} = -0.07$ ($M_{\text{ORB}}^{\text{Fe}} = -0.008$) in $\text{Ce}_2\text{ZrFe}_{15}$ increases to 0.142 (0.03) for 60% Co doping (in $\text{Ce}_2\text{Fe}_6\text{Co}_9\text{Zr}$). Both $M_{\text{ORB}}^{\text{Ce}}$ and $M_{\text{ORB}}^{\text{Fe}}$ exhibits a non monotonic dependence Co concentration, and exhibit maxima at 40%, and 60% doping, respectively. According to Bruno's theorem⁴⁹ the MAE is directly proportional to anisotropy of orbital magnetic moment, and can be described as $\text{MAE} = \sum_i \Delta M_{\text{ORB}}^i \Lambda_{\text{SOC}}^i S_i$. Here Λ_{SOC}^i , ΔM_{ORB}^i , and S_i refer to the spin-orbital coupling constant, anisotropy of orbital moments, and spin moment of atomic site i . As suggested by Bruno's formula, the MAE (Figure 2(b)) and orbital moments anisotropy exhibit (Figure 5) nearly the same dependence on Co concentration. If the interaction between Ce, and transition metal sub lattice can be ignored, the MAE can be linearly expanded in term of Ce and transition metal sub lattice. Given that the strength of SOC for $4f$ rare-earth elements is order of magnitude larger than that Fe/Co, it indicates that a sizable fraction of the MAE will originate from Ce site. At the same time the substantial $M_{\text{ORB}}^{\text{Fe/Co}}$ suggests that, Fe/Co will also have some valuable contribution to MAE. This is in accord with the substantial uniaxial anisotropy of CaCu_5 structure materials such as LaCo_5 and YCo_5 , which entirely lack the $4f$ electrons usually believed to create large magnetic anisotropies⁵⁰.

The magnetic properties calculated above show substantial potential for application as permanent magnets. However as shown in previous studies VCA can overestimate the MAE^{51,52}. Therefore, to confirm the improved MAE under Co alloying calculations have also been performed by modeling Co doping within a super-cell approach^{52,53}. The Fe atoms were replaced by Co atoms to form the various $\text{Ce}_2\text{ZrFe}_{15-x}\text{Co}_x$ type alloy compositions. In total 4 alloy compositions were studied by replacing 3, 6, 9, and 12 Fe atoms by Co. Due to the large number of inequivalent atomic site, utilizing a super-cell based method for MAE calculation is a computationally expensive task. Hence, we study only the cells where the rhombohedral symmetry was preserved. For this purpose, the sites for Co doping were selected such that the crystallographic site symmetry was preserved. This procedure results in one, two, two, and one configuration for 20, 40, 60, and 80% Co doping. After Co substitution, atomic positions in all the structures were relaxed until forces were less than 1 mRy/Bohr. Subsequently the lowest energy structure (for 40, and 60% Co doping case) was used for magnetic property calculations, which are shown in Figure 6(a). For the 60% Co case we identify as the optimal alloy, this structure is some 100 meV lower than the other considered structure so that this structure is significantly favored energetically. The total magnetic moments and MAE for $\text{Ce}_2\text{ZrFe}_{15-x}$ as a function of x calculated within super-cell approach are shown in Figure 6(b), and Figure 6(c), respectively. Here the results obtained within VCA method are also shown for comparison. As expected both super-cell and VCA method produce nearly the same magnetic moments. The situation however, is somewhat different for MAE, where we see that MAE switches from planar to uniaxial at 60% Co doping, as opposed to 40% as observed with VCA method. Within super-cell method at 60% Co doping the calculated MAE is $\sim 5.8 \text{ MJ/m}^3$, a bit

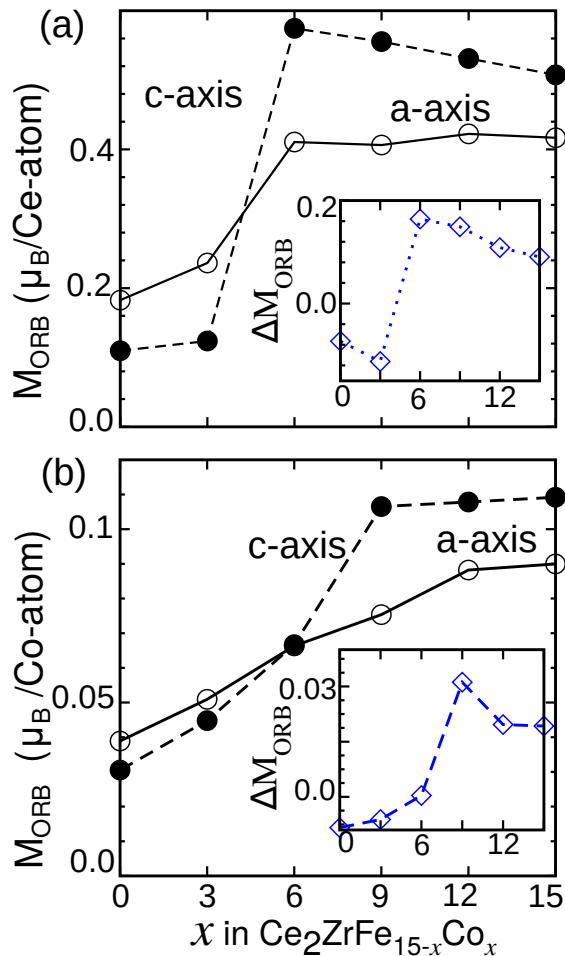


FIG. 5. (a) The orbital magnetic moment M_{ORB} (a) for Ce sites, and (b) for Co/Fe sites as a function of x in $Ce_2ZrFe_{15-x}Co_x$ calculated under GGA+SOC+U. The insets give the anisotropy of orbital magnetic moment ($\Delta M_{ORB} = M^c - M^a$).

smaller than the VCA value of 7.78 MJ/m^3 . Nonetheless, for 60% and higher Co concentration, the calculated MAE within super-cell and VCA method are in reasonable agreement. The total magnetization and MAE calculated with no U are also shown in Figures 6(a), and (b) by green dashed line (open diamonds). Similar to the VCA case, while the calculated MAE with no U is relatively smaller than $U_{Ce} = 3\text{eV}$, it is sufficiently large (4.17 MJ/m^3 for 60% Co doping) to yield a high performance permanent magnet.

To get insight into the stability of these alloys we also computed the formation energy (E^{form}) with respect to elemental decomposition, which are listed in Table I. We observe that all compounds studied here have negative formation energy, indicating that all alloys are stable against the elemental decomposition. Among the system explored here Ce_2ZrFe_{15} shows the least formation energy of -44 meV/atom , whereas the formation energy of Ce_2ZrCo_{15} is -112 meV/atom . Interestingly, with increasing x (Co concentration) in $Ce_2ZrFe_{15-x}Co_x$ the and at $x=9$ (at 60% Co doping) it becomes -110 meV/atom ; comparable to Ce_2ZrCo_{15} . This finding of substantial neg-

ative formation energy on the Co-rich side of the alloy is a strong indication of the likely experimental feasibility of synthesis of these compounds.

One may make a projection of the potential energy product BH_{max} of suitably optimized alloys in this family from these results. The $T=0$ magnetization M_s of our $Ce_2Fe_6Co_9Zr$ alloy, at $27.15 \mu_B$ per formula unit, on a volumetric basis is some 1.26 Tesla. Given the calculated magnetic anisotropy constant K_1 of 7.78 MJ/m^3 , the magnetic hardness parameter $\kappa = K_1/\mu_0 M_s^2$ takes the value $\kappa = 6.19 \gg 1$, indicating that the maximum possible energy product $M_s^2/4$, or 40 MG-Oe, should be achievable at low temperature. At the technologically relevant room temperature, with a slightly smaller moment this value would be closer to 32 MG-Oe, assuming a 10 percent reduction in M_s at room temperature. While we make no detailed study of the Curie point of these alloys, previous work finds the Curie point of Zr-alloyed Ce_2Co_{17} ^{10,12} to be of order 900 K, so that we anticipate only a small magnetization reduction due to temperature effects.

There is a compensating factor, however, that makes the 300 K achievable performance in this alloy system more probably the original 40 MG-Oe figure. The κ value quoted above, deriving largely from the distortion of the 2-17 structure towards the 1-5 structure by Zr, is sufficiently large that smaller concentrations of Zr than the full substitution (approximately 7.5 percent by weight) modeled here may well produce optimal performance. This is in fact known from previous work on Sm_2Co_{17} -based magnets, for which typical mass concentrations of magnets in actual usage are of order 3 weight percent⁵⁴. As noted above, Zr (due largely to its substituting for two $3d$ atoms) has a disproportionate effect on the magnetic moment, and so one may envision an alloy composed of effectively equal proportions of our $Ce_2Fe_6Co_9Zr$ considered in detail here and $Ce_2(Fe_{0.4}Co_{0.6})_{17}$ as a means of simulating lower Zr content. Since magnetic anisotropy is generally an atomic-level quantity, we may consider that the magnetic anisotropy of such an alloy should be approximately the mean of these two quantities, which we find to be 3.6 MJ/m^3 , so that one still finds sufficient magnetic anisotropy for a strong permanent magnet. One may make a similar argument concerning the magnetization, and we find from direct calculation the magnetization of $Ce_2(Fe_{0.4}Co_{0.6})_{17}$ to be some $32.5 \mu_B/\text{formula unit}$, so that the magnetization of our lower-Zr alloy (averaging these two components) would be some 1.4 T at low temperature, or likely approximately 1.26 T or larger at room temperature. One would then recover the original potential energy product of this alloy of 40 MG-Oe, but at room temperature. As with present SmCo-based magnets, the much higher likely Curie point than $Nd_2Fe_{14}B$ (585 K) means that above room temperature these magnets would likely outperform Nd-based magnets by a substantial margin.

IV. CONCLUSIONS

By performing first principles calculations we carry out a detailed study of the magnetic properties of Ce_2Fe_{17} , and Ce_2Co_{17} under Zr substitution at the dumbbell site. While

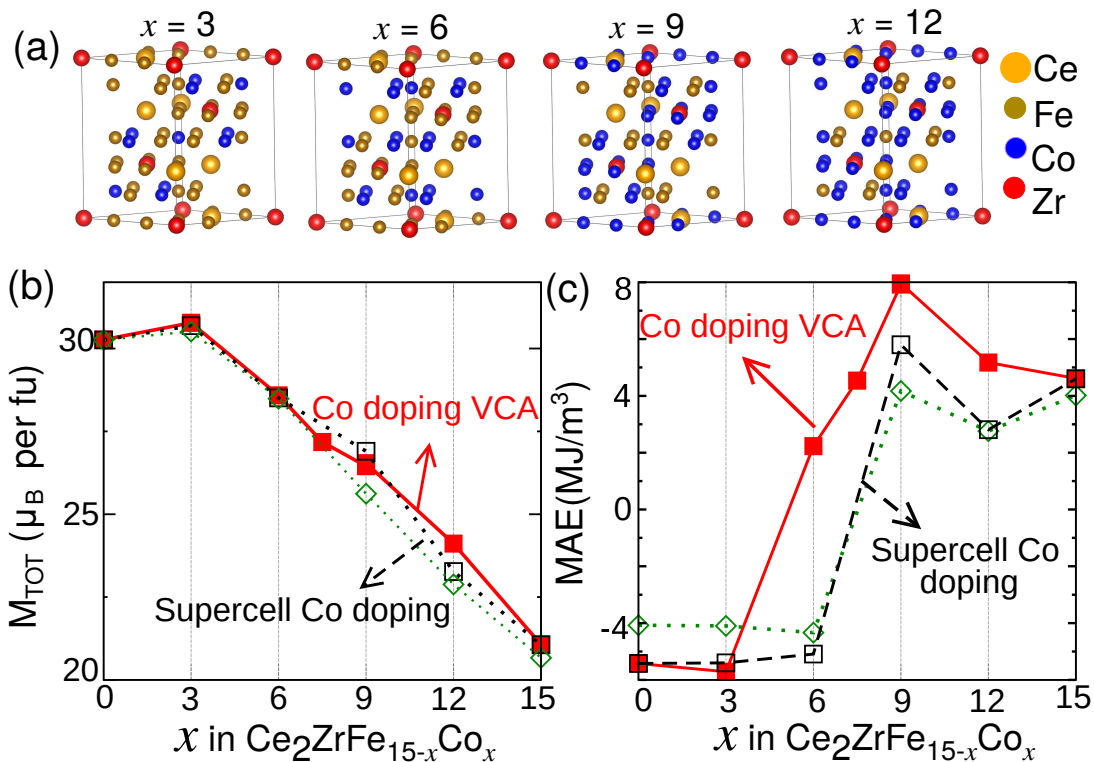


FIG. 6. (a) The configuration used to model 20, 40, 60, and 80% Co doping via super-cell method. (b) Total magnetic (spin + orbital) moment and (c) magnetic anisotropy energy calculated under GGA+SOC+U as function of x in $\text{Ce}_2\text{ZrFe}_{15-x}\text{Co}_x$. Symbols correspond to the calculated compositions, and line is a guide to eye. Results from VCA calculations are also shown for comparison. The results from without Hubbard U calculations are shown in green open diamonds.

we find that Zr doping has no favorable effect on the MAE of $\text{Ce}_2\text{Fe}_{17}$, consistent with previous reports, for $\text{Ce}_2\text{Co}_{17}$ we show that MAE can be significantly improved by one Zr substitution at Co_2 dumbbell site. In order to further improve the magnetic properties, the total magnetization and MAE were calculated, at a few selected concentrations between $\text{Ce}_2\text{Fe}_{15}\text{Zr}$ and $\text{Ce}_2\text{Co}_{15}\text{Zr}$ within the VCA method. We show that the MAE can be significantly tuned by varying the Co concentration, and switches from planar to uniaxial at 40 % Co doping. The calculated MAE, exhibits a strong dependence on Co concentration, and peaks at 60 % Co doping (in $\text{Ce}_2\text{Fe}_9\text{Co}_6\text{Zr}$), which is more than two times higher than the MAE value calculated in end compound $\text{Ce}_2\text{Co}_{15}\text{Zr}$. Very importantly $\text{Ce}_2\text{Fe}_9\text{Co}_6\text{Zr}$ still maintains a relatively high value of saturation magnetization (~ 1.3 times higher than of $\text{Ce}_2\text{Co}_{15}\text{Zr}$). These calculations suggests the 60% Co Zr-alloyed material has potential room temperature energy products as high as 40 MG-Oe and likely better temperature dependence than $\text{Nd}_2\text{Fe}_{14}\text{B}$. By analyzing the electronic density of states, we assess that the switching of MAE from planar

to uniaxial in $\text{Ce}_2\text{ZrFe}_{15-x}\text{Co}_x$, is likely related to Ce valence fluctuations in these compounds. This is further corroborated by the observed enhancement in Ce spin and orbital magnetic moments. We hope that our current theoretical findings will stimulate experimental exploration of the magnetic properties of Zr and Fe-alloyed $\text{Ce}_2\text{Co}_{17}$ alloys.

V. ACKNOWLEDGMENT

This research was supported by the Critical Materials Institute, an Energy Innovation Hub funded by the U.S. Department of Energy, Office of Energy Efficiency and Renewable Energy, Advanced Manufacturing Office. This research used resources of the Compute and Data Environment for Science (CADES) at the Oak Ridge National Laboratory, which is supported by the Office of Science of the U.S. Department of Energy under Contract No. DE-AC05-00OR22725. The Department of Energy will provide public access to these results of federally sponsored research in accordance with the DOE Public Access Plan⁵⁵.

* This manuscript has been authored by UT-Battelle, LLC under Contract No. DE-AC05-00OR22725 with the U.S. Department

of Energy. The United States Government retains and the publisher, by accepting the article for publication, acknowledges that

- the United States Government retains a non-exclusive, paid-up, irrevocable, world wide license to publish or reproduce the published form of this manuscript, or allow others to do so, for United States Government purposes. The Department of Energy will provide public access to these results of federally sponsored research in accordance with the DOE Public Access Plan (<http://energy.gov/downloads/doe-public-access-plan>).
- ¹ M. A. Susner, B. S. Conner, B. I. Saparov, M. A. McGuire, E. J. Crumlin, G. M. Veith, H. Cao, K. V. Shanavas, D. S. Parker, B. C. Chakoumakos, *et al.*, 2Flux growth and characterization of Ce-substituted Nd₂Fe₁₄B single crystals, *J. Magn. Magn. Mater.* **434**, 1 (2017).
 - ² B. Conner, M. McGuire, K. Shanavas, D. Parker, and B. Sales, Evolution of structural and magnetic properties in La_xCe_{2-x}Co₁₆Ti for $0 \leq x \leq 2$, *J. Alloys Compd.* **695**, 2266 (2017).
 - ³ J. Jin, Y. Zhang, G. Bai, Z. Qian, C. Wu, T. Ma, B. Shen, and M. Yan, Manipulating Ce valence in RE₂Fe₁₄B tetragonal compounds by La-Ce co-doping: Resultant crystallographic and magnetic anomaly, *Sci. Rep* **6**, 30194 (2016).
 - ⁴ T. Pandey, M.-H. Du, and D. S. Parker, Tuning the Magnetic Properties and Structural Stabilities of the 2-17-3 Magnets Sm₂Fe₁₇X₃ (X = C, N) by Substituting La or Ce for Sm, *Phys. Rev. Appl.* **9**, 034002 (2018).
 - ⁵ T. N. Lamichhane, V. Taufour, A. Palasyuk, Q. Lin, S. L. Budko, and P. C. Canfield, Ce_{3-x}Mg_xCo₉: Transformation of a Pauli paramagnet into a strong permanent magnet, *Phys. Rev. Appl.* **9**, 024023 (2018).
 - ⁶ T. Pandey and D. S. Parker, Borderline Magnetism: How Adding Mg to Paramagnetic CeCo₃ Makes a 450-K Ferromagnet with Large Magnetic Anisotropy, *Phys. Rev. Appl.* **10**, 034038 (2018).
 - ⁷ M. Bartashevich, T. Goto, R. Radwanski, and A. Korolyov, Magnetic anisotropy and high-field magnetization process of CeCo₅, *J. Magn. Magn. Mater* **131**, 61 (1994).
 - ⁸ T. N. Lamichhane, M. T. Onyszczak, O. Palasyuk, S. Sharikadze, T.-H. Kim, Q. Lin, M. J. Kramer, R. McCallum, A. L. Wysocki, M. C. Nguyen, *et al.*, Single-Crystal Permanent Magnets: Extraordinary Magnetic Behavior in the Ta-, Cu-, and Fe-Substituted CeCo₅ Systems, *Phys. Rev. Appl.* **11**, 014052 (2019).
 - ⁹ R. Streever, Individual Co site contributions to the magnetic anisotropy of RCo₅ compounds and related structures, *Phys. Rev. B* **19**, 2704 (1979).
 - ¹⁰ H. Fujii, M. Satyanarayana, and W. Wallace, Magnetic and crystallographic properties of substituted Ce₂Co_{17-x}T_x compounds (T= Ti, V, Cr, Mn, Fe, Cu, Zr, and Hf), *J. Appl. Phys.* **53**, 2371 (1982).
 - ¹¹ Z.-g. Sun, S.-y. Zhang, H.-w. Zhang, J.-y. Wang, and B.-g. Shen, The effect of manganese substitution on the magnetic properties of Ce₂Co₁₇ compounds, *J. Phys. Condens. Matter* **12**, 2495 (2000).
 - ¹² H. Fujii, M. Satyanarayana, and W. Wallace, Effect of substitution of Zr on the magnetic properties of R₂Co₁₇ (R= Ce and Sm), *Solid State Commun.* **41**, 445 (1982).
 - ¹³ X. Wei, S. Hu, D. Zeng, X. Kou, Z. Liu, E. Brück, J. Klaasse, F. De Boer, and K. Buschow, Structure and magnetic properties of Ce₂Co_{17-x}Si_x compounds, *Physica B: Condensed Matter* **262**, 306 (1999).
 - ¹⁴ S. Hu, X. Wei, D. Zeng, X. Kou, Z. Liu, E. Brück, J. Klaasse, F. De Boer, and K. Buschow, Structure and magnetic properties of Ce₂Co_{17-x}Al_x compounds, *J. Alloys Compd.* **283**, 83 (1999).
 - ¹⁵ B.-g. Shen, Z.-h. Cheng, S.-y. Zhang, J.-y. Wang, B. Liang, H.-w. Zhang, and W.-s. Zhan, Magnetic properties of R₂Co₁₅Al₂ compounds with R= Y, Ce, Pr, Nd, Sm, Gd, Tb, Dy, Ho, Er, and Tm, *J. Appl. Phys.* **85**, 2787 (1999).
 - ¹⁶ P. Larson and I. Mazin, Effect of lattice relaxation on magnetic anisotropy: Zr-doped Sm₂Co₁₇, *Phys. Rev. B* **69**, 012404 (2004).
 - ¹⁷ L. Ke, D. Kukusta, and D. D. Johnson, Origin of magnetic anisotropy in doped Ce₂Co₁₇ alloys, *Phys. Rev. B* **94**, 144429 (2016).
 - ¹⁸ D. Singh, *Planes Waves, Pseudopotentials and the LAPW* (Method, Kluwer Academic, 1994).
 - ¹⁹ E. Sjöstedt, L. Nordström, and D. Singh, An alternative way of linearizing the augmented plane-wave method, *Solid State Commun.* **114**, 15 (2000).
 - ²⁰ P. Blaha, K. Schwarz, G. K. H. Madsen, D. Kvasnicka, and J. Luitz, *WIEN2K, An Augmented Plane Wave + Local Orbitals Program for Calculating Crystal Properties* (Karlheinz Schwarz, Techn. Universität Wien, Austria, 2001).
 - ²¹ L. Vegard, Die Konstitution der Mischkristalle und die Raumbfüllung der Atome, *Zeitschrift für Physik* **5**, 17 (1921).
 - ²² A. R. Denton and N. W. Ashcroft, Vegard's law, *Phys. Rev. A* **43**, 3161 (1991).
 - ²³ J. P. Perdew, K. Burke, and M. Ernzerhof, Generalized gradient approximation made simple, *Phys. Rev. Lett.* **77**, 3865 (1996).
 - ²⁴ D. D. Koelling and B. N. Harmon, A technique for relativistic spin-polarised calculations, *Journal of Physics C: Solid State Physics* **10**, 3107 (1977).
 - ²⁵ H. Lu and L. Huang, Pressure-driven 4 f localized-itinerant crossover in heavy-fermion compound cein 3: A first-principles many-body perspective, *Phys. Rev. B* **94**, 075132 (2016).
 - ²⁶ H. Lu and L. Huang, Itinerant-localized crossover and orbital dependent correlations for 4 f electrons in cerium-based ternary 122 compounds, *Phys. Rev. B* **98**, 195102 (2018).
 - ²⁷ W. Temmerman, L. Petit, A. Svane, Z. Szotek, M. Lüders, P. Strange, J. Staunton, I. Hughes, and B. L. Gyorffy, *Handbook on the physics and chemistry of rare earths* **39**, 1 (2009).
 - ²⁸ V. I. Anisimov, J. Zaanen, and O. K. Andersen, Band theory and mott insulators: Hubbard u instead of stoner i, *Phys. Rev. B* **44**, 943 (1991).
 - ²⁹ A. Svane, Electronic structure of cerium in the self-interaction corrected local spin density approximation, *Phys. Rev. Lett.* **72**, 1248 (1994).
 - ³⁰ A. Svane, W. Temmerman, and Z. Szotek, Theory of pressure-induced phase transitions in cerium chalcogenides, *Phys. Rev. B* **59**, 7888 (1999).
 - ³¹ V. I. Anisimov, I. Solovyev, M. Korotin, M. Czyżyk, and G. Sawatzky, Density-functional theory and NiO photoemission spectra, *Phys. Rev. B* **48**, 16929 (1993).
 - ³² A. Liechtenstein, V. Anisimov, and J. Zaanen, Density-functional theory and strong interactions: Orbital ordering in Mott-Hubbard insulators, *Phys. Rev. B* **52**, R5467 (1995).
 - ³³ I. Solovyev, P. Dederichs, and V. Anisimov, Corrected atomic limit in the local-density approximation and the electronic structure of d impurities in Rb, *Phys. Rev. B* **50**, 16861 (1994).
 - ³⁴ D. Givord and R. Lemaire, Magnetic transition and anomalous thermal expansion in R₂Fe₁₇ compounds, *IEEE Transactions on Magnetics* **10**, 109 (1974).
 - ³⁵ D. Middleton and K. Buschow, Magnetic properties of Ce₂Fe_{17-x}Si_x compounds, *J. Alloys Compd* **206**, L1 (1994).
 - ³⁶ S. R. Mishra, G. J. Long, O. A. Pringle, D. Middleton, Z. Hu, W. B. Yelon, F. Grandjean, and K. Buschow, A magnetic, neutron diffraction, and Mössbauer spectral study of the Ce₂Fe_{17-x}Al_x solid solutions, *J. Appl. Phys.* **79**, 3145–3155 (1996).
 - ³⁷ Y. Janssen, S. Chang, A. Kreyssig, A. Kracher, Y. Mozharivskyy, S. Misra, and P. Canfield, Magnetic phase diagram of Ce₂Fe₁₇, *Phys. Rev. B* **76**, 054420 (2007).
 - ³⁸ A. Teplykh, A. Pirogov, and A. Kuchin, Magnetic structure of Ce₂Fe_{17-x}Mn_x intermetallic compounds, *Phys. Solid State* **52**,

- 922 (2010).
- ³⁹ See Supplemental Material at <http://link.aps.org/supplemental>.
- ⁴⁰ X. Xu and S. A. Shaheen, Structural and magnetic properties of rare earth iron nitride series $R_2(\text{Fe}_{1-x}\text{Co}_x)_{17}\text{N}_{3-\delta}$, *J. Appl. Phys.* **73**, 1892 (1993).
- ⁴¹ R. K. Chouhan and D. Paudyal, Cu substituted CeCo_5 : New optimal permanent magnetic material with reduced criticality, *J. Alloys Compd.* **723**, 208 (2017).
- ⁴² O. Isnard, S. Miraglia, D. Fruchart, C. Giorgetti, E. Dartyge, and G. Krill, X-ray absorption spectroscopy and magnetic circular x-ray dichroism in $\text{Ce}_2\text{Fe}_{17}\text{N}_3$, *J. Phys. Condens. Matter* **8**, 2437 (1996).
- ⁴³ O. Isnard, S. Miraglia, C. Giorgetti, E. Dartyge, G. Krill, and D. Fruchart, Ce valence state probed by XAFS study in $\text{Ce}_2\text{Fe}_{17-x}\text{Ga}_x\text{H}_y$ compounds, *J. Alloys Compd.* **262**, 198 (1997).
- ⁴⁴ J. Coey, J. Allan, A. Minakov, and Y. V. Bugaslavsky, $\text{Ce}_2\text{Fe}_{17}$: Mixed valence or 4 f band? *J. Appl. Phys.* **73**, 5430 (1993).
- ⁴⁵ R. Neifeld, M. Croft, T. Mihalisin, C. Segre, M. Madigan, M. Torikachvili, M. Maple, and L. DeLong, Chemical environment and Ce valence: Global trends in transition-metal compounds, *Phys. Rev. B* **32**, 6928 (1985).
- ⁴⁶ B. C. Sales, A model for the thermodynamic properties of metallic rare earth systems with an unstable valence, *J. Low Temp. Phys.* **28**, 107 (1977).
- ⁴⁷ B. Sales and D. Wohlleben, Susceptibility of interconfiguration-fluctuation compounds, *Phys. Rev. Lett.* **35**, 1240 (1975).
- ⁴⁸ A. Alam and D. D. Johnson, Mixed valency and site-preference chemistry for cerium and its compounds: A predictive density-functional theory study, *Phys. Rev. B* **89**, 235126 (2014).
- ⁴⁹ P. Bruno, Tight-binding approach to the orbital magnetic moment and magnetocrystalline anisotropy of transition-metal monolayers, *Phys. Rev. B* **39**, 865 (1989).
- ⁵⁰ L. Steinbeck, M. Richter, and H. Eschrig, Magnetocrystalline anisotropy of RCO_5 intermetallics: itinerant-electron contribution, *J. Magn. Magn. Mater.* **226**, 1011 (2001).
- ⁵¹ A. Edström, M. Werwiński, D. Iuşan, J. Ruzs, O. Eriksson, K. Skokov, I. Radulov, S. Ener, M. Kuzmin, J. Hong, *et al.*, Magnetic properties of $(\text{Fe}_{1-x}\text{Co}_x)_2\text{B}$ alloys and the effect of doping by 5d elements, *Phys. Rev. B* **92**, 174413 (2015).
- ⁵² S. Steiner, S. Khmelevskiy, M. Marsmann, and G. Kresse, Calculation of the magnetic anisotropy with projected-augmented-wave methodology and the case study of disordered $\text{Fe}_{1-x}\text{Co}_x$ alloys, *Phys. Rev. B* **93**, 224425 (2016).
- ⁵³ M. Däne, S. K. Kim, M. P. Surh, D. Åberg, and L. X. Benedict, Density functional theory calculations of magnetocrystalline anisotropy energies for $(\text{Fe}_{1-x}\text{Co}_x)_2\text{B}$, *J. Phys. Condens. Matter* **27**, 266002 (2015).
- ⁵⁴ J. Ormerod, Personal communication.
- ⁵⁵ <https://www.energy.gov/downloads/doe-public-access-plan>.